 CMES, vol.52, no.3, pp.279-295, 2009

Contact between a Tunnel Lining and a Damage-Susceptible Viscoplastic Medium

Frederic L. Pellet[1]

Abstract: In this study, the contact and interaction between a tunnel lining support and a damage-susceptible viscoplastic medium is investigated. First, back-analysis of the time-dependent behaviour of a drift excavated across a carboniferous rock mass which exhibited large delayed displacements was undertaken. Drift closure was simulated using an elasto-viscoplastic constitutive model that included the strength degradation process. This 3D numerical simulation was performed taking into account both stage construction sequence and rate of excavation advancement. A comparison of the numerical results with the data measured on site allowed for the calibration of the model parameters. Subsequently, the installation of a concrete lining was simulated to account for contact with the rock mass. This blind numerical simulation aimed to optimize the tunnel cross-section and establish the dimensions of a suitable concrete supporting lining. Three months after installation, the stresses measured in the concrete lining were in agreement with the numerically predicted stresses.

Keywords: Damage, viscoplasticity, tunnel support, soil structure interaction, soft rock.

1 Introduction

In geotechnical engineering, soil and rock masses often need to be supported by structural elements to prevent collapse or instability. The contact between structural elements and the surrounding medium is therefore of primary importance and appropriate numerical simulations are required in order to optimize the construction sequences and the establishment of the dimensions of the lining support.

In this paper we present a case study of the interaction between a tunnel lining and the surrounding rock mass, which has experienced large time-dependent displacements due to rock creep and damage.

[1] University of Grenoble, Laboratory 3S-R, Grenoble, France

Several authors have studied this phenomenon, for example, Kropik and Mang (1996); Boidy et al. (2002); Dhawan et al. (2002); Sandrone et al. (2006); Sterpi and Gioda (2009), Pellet et al. (2009). However, there is still a lack of knowledge especially when comparing numerical results to measured field data. Therefore additional investigations are needed to validate the numerical simulation of the observed behaviour of soft rocks.

From a more theoretical point of view, this problem raises different questions related to advanced numerical modelling such as 3D analysis (Tan et al. 2009, Sladek et al. 2009), large deformation computations (Dinis et al. 2009) or rate-dependent damage (Luming, 2009).

2 Presentation of the encountered drift

2.1 Geological context and construction process

The tunnel under study was a drift excavated for a high speed railway project, linking France to Italy across the Alps (Triclot et al., 2007). During the drift excavation, a highly fractured carboniferous rock formation was encountered. In this formation, at 300 meters depth, large displacements of the tunnel wall, of about 0.9 meter, were observed. The drift was subsequently re-excavated and the concrete lining support system was modified as reported by Rettighieri et al. (2008).

Due to the nature of the geological formations it was foreseen that the principal difficulties in the tunnel excavation would be due to:

- High overburden stress in the highly disturbed and tectonised geological formation,
- Rocks prone to creep with poor mechanical properties (soft rocks),

The drift was carried out in the following sequence:

- 5-meter long sections were excavated using the “drill and blast” method,
- light temporary supports made of shotcrete, rock bolts, and steel sets were installed,
- the next section of excavation was undertaken.

The time to complete each cycle was approximately 5 days; thus the average advancement rate was 1 meter per day.

2.2 Characterization of the mechanical properties of the rock mass

The mechanical properties of the rock, both elastic and plastic, were assessed based on laboratory tests (triaxial compression tests) and in-situ investigations (Russo, 2009). For the latter tests, rock mass classifications such as GSI (Geological Strength Index) and RMR (Rock Mass Rating) were used to calibrate the Hoek and Brown failure criterion (equation 1) parameters at the scale of the rock mass.

$$\sigma_1 = \sigma_3 + \sigma_{ci}\left(m\frac{\sigma_1}{\sigma_{ci}} + s\right)^a \tag{1}$$

where: σ_1 is the principal stress
σ_3 is the minor principal stress
σ_{ci} is the unconfined compressive strength of the intact rock
m, s, and a are the model parameters

Using the suggested method (ISRM, 2007), the following set of values for the peak strength and for the residual strength were obtained (Table 1).

Table 1: Parameters for generalized Hoek and Brown failure criterion

Intact rock	**Rock mass: peak values**	**Rock mass: residual values**
m_i = 7	m_b=0.687	m_r =0.481
σ_{ci} = 20 MPa	s = 0.00073	s = 0.00024
	a = 0.516	a = 0.531

2.3 Data from tunnel monitoring

During the drift construction an extensive monitoring program was undertaken (Triclot et al. 2007; Rettighieri et al. 2008). Variations in the tunnel diameter, or tunnel convergence, were measured, and extensometers were used to measure displacements inside the rock mass in the vicinity of the drift.

For the purpose of this study, three cross-sectional areas were selected. Figure 1 shows the radial displacement of the tunnel wall versus time as well as the face advancement of the excavation for all three sections (Russo et al. 2009). The maximum displacement was almost 90 cm after about 100 days. It should be noted that the displacements increased with time even when the excavation stopped. Later, this time span will be used to calibrate the rock rheological parameter.

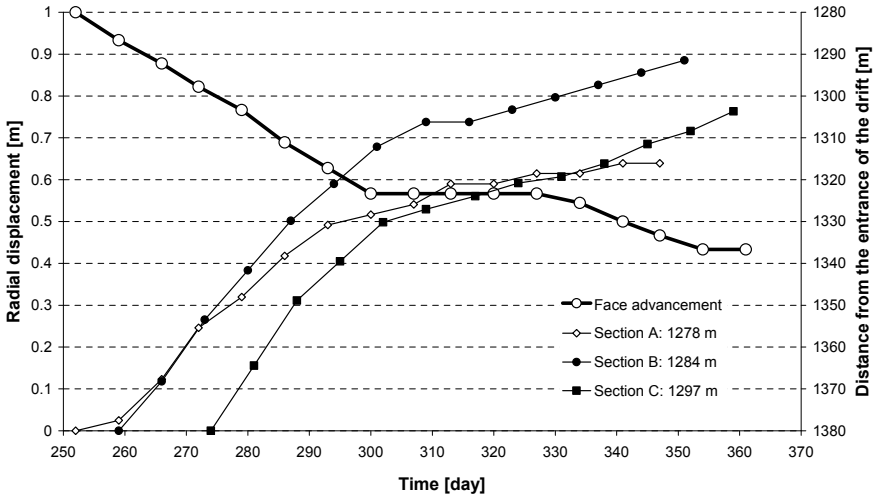

Figure 1: Measurements of wall displacements at different sections with respect to time and face advancement. Sections were located at 1284, 1278 and 1297 meters from the tunnel entrance

3 Numerical modelling of drift excavation

In order to tackle the problem of large delayed displacements within the drift, a 3D model using the finite difference numerical code, FLAC 3D, was run. This code was selected mainly because it allows for large displacements to be taken into account. Due to the explicit scheme of resolution precautions needed to be taken when choosing the critical time steps (Marti and Cundall 1980; Cormeau, 1975).

The objective of the numerical simulation was to optimize the tunnel cross-section in order to establish the dimensions of a suitable supporting system.

3.1 Geometrical model, stages of calculations and constitutive model

3.1.1 Geometrical model and boundary conditions

The geometrical model for the drift was a block of 105 m in length, 80 m in height and 50 m in width (Figure 2). The boundary and the initial conditions were taken as follows:

- Zero normal displacements at the lower face and the rear face of the model as well as at the symmetry plane,
- An initial stress of 7.5 MPa on the other three faces of the model.

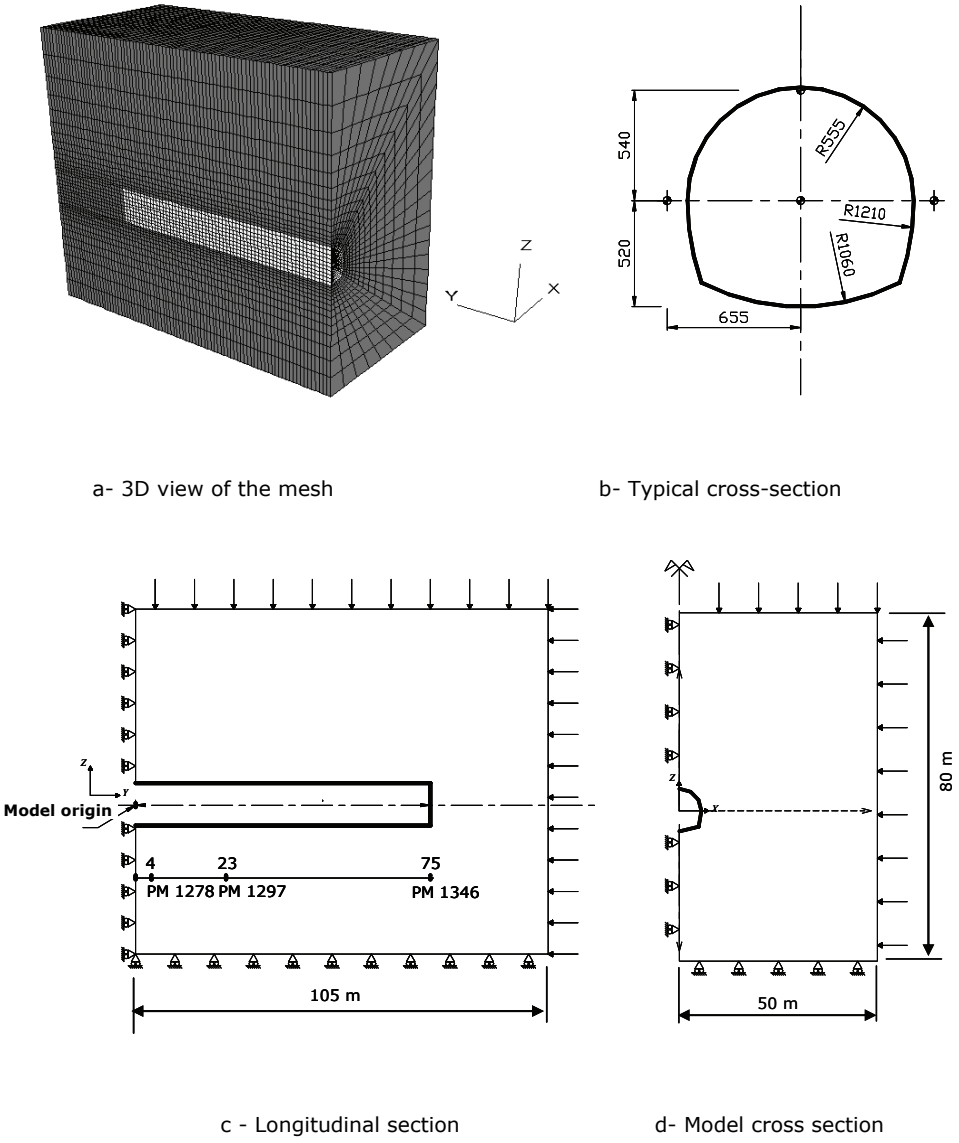

a- 3D view of the mesh

b- Typical cross-section

c - Longitudinal section

d- Model cross section

Figure 2: Model dimensions and boundary conditions

3.1.2 CVISC constitutive model

Based on the experimental data it was obvious that the chosen constitutive model has to be capable of computing both instantaneous strains and time-dependent

strains including strength degradation or damage. Several authors (Selvadurai, 2004; Pellet et al. 2005) have proposed models to handle this problem.

For this study we chose to use the CVISC constitutive model which allows for the computation of both instantaneous and delayed deviatoric strains (Boidy et al., 2002). Instantaneous strains are computed using an elasto-plastic constitutive model involving a Mohr-Coulomb failure criterion. Therefore it requires two elastic parameters (the elastic modulus, E, and shear modulus, G) and three plastic parameters (the dilatation angle ψ, friction angle Φ and cohesion c).

For time-dependent behaviour, a Burger visco-plastic model is coupled to the elasto-plastic model. The Burger model is composed of a Kelvin unit for primary creep (transient creep) and a Maxwell unit for secondary or stationary creep. Two parameters are required for the Kelvin unit (Kelvin viscosity and Kelvin stiffness) and two for the Maxwell unit (Maxwell viscosity and Maxwell stiffness).

The last feature required is the time-dependent damage, which will simulate strength degradation with respect to time (tertiary creep). In the model, cohesion was decreased from 100% to 25%. The evolution law was calibrated versus the data provided by Russo (2009).

The rheological units for the CVISC constitutive model are shown in Figure 3 and the constitutive equation is written as follows:

$$\eta_K * \ddot{\gamma} + G_K * \dot{\gamma} = \eta_K * \frac{\ddot{\tau}}{E_M} + \dot{\tau} * \left(1 + \frac{\eta_K}{\eta_M} + \frac{E_K}{E_M}\right) + \tau * \frac{E_K}{\eta_M} \tag{2}$$

where: τ is the shear stress,
γ is the distorsion (shear strain),
η_M is the Maxwell viscosity,
η_K is the Kelvin viscosity,
G_K is the Kelvin shear modulus,
E_M is the Maxwell modulus,
E_K is the Kelvin modulus.

3.1.3 Stages of computation

After stress initialization in the model, excavation was simulated in 5-m long sections of 5 meter length. For each excavation stage, computation begins with an elastoplastic analysis. As soon as the model equilibrium is reached, the creep model is activated for a time span of five days. The sequence is reiterated until the model is fully excavated.

It should be mentioned that the creep model utilizes a routine for the management of time steps based on the ratio of unbalanced forces. Technically, this time step varied between 2.5 10^{-3} day (216 s) to 5 10^{-2} day (4320 s).

3.2 Back-analysis of convergence data for constitutive parameter calibration

3.2.1 Computational steps and calibration

One of the main difficulties for this type of numerical simulation is the selection of representative values of the different constitutive parameters. Indeed, there is a scale effect and the in situ characteristics differ from those measured in the laboratory (Han-Ping-Chin and Rogers, 1987; Korzeniowski, 1991; Fabre and Pellet, 2006). Therefore, the first step of the computation was to back-analyse the time-dependent behaviour of the drift based on the monitoring data. This was done in order to constrain and to calibrate the parameters of the constitutive model used to simulate the mechanical behaviour of the rock mass.

Instantaneous properties were calibrated using both the analytical solution and numerical model; they are the Maxwell properties, namely the Maxwell shear modulus, G_M, and the Maxwell modulus, E_M (Figure 3). Time-dependent characteristics were constrained using an analytical equation (Sulem et al., 1987).

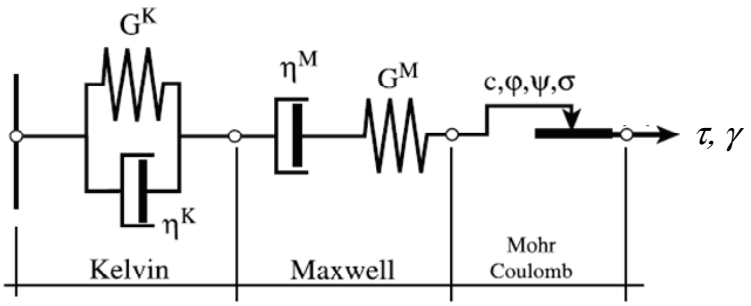

Figure 3: Rheological units for CVISC constitutive model

The Mohr-Coulomb peak characteristics were deduced from the Hoek and Brown criterion, which was itself calibrated using the Geological Strength Index (ISRM, 2007). Viscosities were given by the convergence curves (i.e. displacements versus time).

The following properties were used in the CVISC model:

- Instantaneous Elastic properties:
  - Maxwell modulus E_M = 1.98 GPa
  - Maxwell shear modulus G_M = 0.76 GPa
- Plastic properties:

- Cohesion c = 0.6 MPa
- Friction angle Φ 26°
- Dilation angle ψ 15°

• Viscoplastic properties:

- Maxwell viscosity η_M = 2.6 10^9 MPa.s
- Kelvin viscosity η_K = 2.6 10^8 MPa.s
- Kelvin modulus G_K = 0.18 MPa

3.2.2 Field of instantaneous displacements

The numerical model provided an instantaneous elastic (reversible) radial displacement of 3.1 cm at a distance from the tunnel face. This maximum value is close to the value obtained from a 2D stress analysis around a circular excavation in plane strain conditions (2.7 cm). The difference between the analytical solution and the numerical results is due to the fact that the state of stress is different; the intermediate principal stress is neglected in the plane strain analysis. Moreover, the non-circular cross section brings in some discrepancy.

The instantaneous plastic displacement profile along the drift axis is shown in the Figure 4 for different positions of the excavation face. The maximum radial displacements are located about 25 cm from the excavation face. One can see from Figure 4 that each excavation stage leads to an uneven profile because of the stress concentration at the junction between the excavation face and the tunnel wall. This stress concentration may initiate the damage and the development of fractures around the tunnel (Eberhardt, 2001; Pellet et al., 2009).

3.2.3 Field of delayed displacements

The evolution of delayed convergences with respect to time was compared to the measured data (Figure 5). The section under consideration was section C (PM 1297). Convergence measurements were recorded every week for different directions. Computed values indicate a jump in the radial displacement after each stage of excavation. These jumps progressively decreased as the distance from the face increased and they completely vanished at a distance of 20 to 25 meters.

A noticeable decrease in the slope of the curves occurred after 5 weeks (35 days). This indicates that the drift face is far from the section under consideration. Therefore the drift face no longer has any influence on the convergence; in other words, the observed deformations were no longer due to the face advancement but to the time-dependent behaviour of the rock mass. It should be noted that the numerical

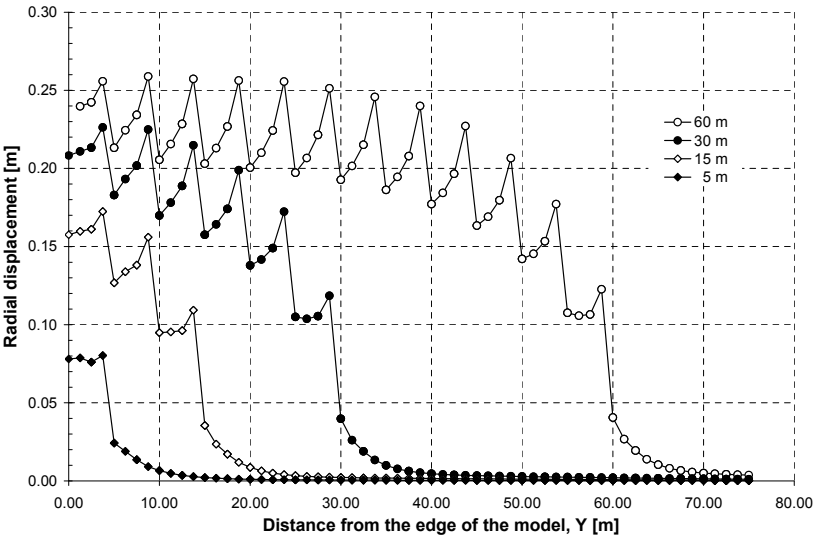

Figure 4: Profile of instantaneous radial displacements along the drift axis for different positions of the excavation face. Stress concentration, located at the junction between the excavation face and tunnel wall leads to a break in the displacement profile.

model underestimates such displacements. The maximum difference was observed for the direction 1-5, where the discrepancy reaches 23 cm at 35 days after the face excavation. At 78 days, this discrepancy was reduced to 16 cm. The difference in the displacement between the different directions is mostly due to the shape of the drift cross section (horse-shoe cross section). The in situ initial state of stress which might be not perfectly isotropic, could also account for some discrepancy.

Overall the comparison between the observed displacements and the numerical results is good, even if the conclusion has to be mitigated because of the high sensitivity of the numerical results to the accuracy of the in situ measurements, which are not easy to achieve in a civil engineering context.

3.3 Lining support installation

As stated in the introduction, large displacements led to the drift closure. Therefore it was necessary to re-excavate the drift cross-section in order to maintain the designed clearance (Rettighieri et al., 2008). Moreover, the installation of a stiff, strong concrete arch lining was required to support the ground pressure.

The numerical simulation was extended to compute the thickness dimensions of

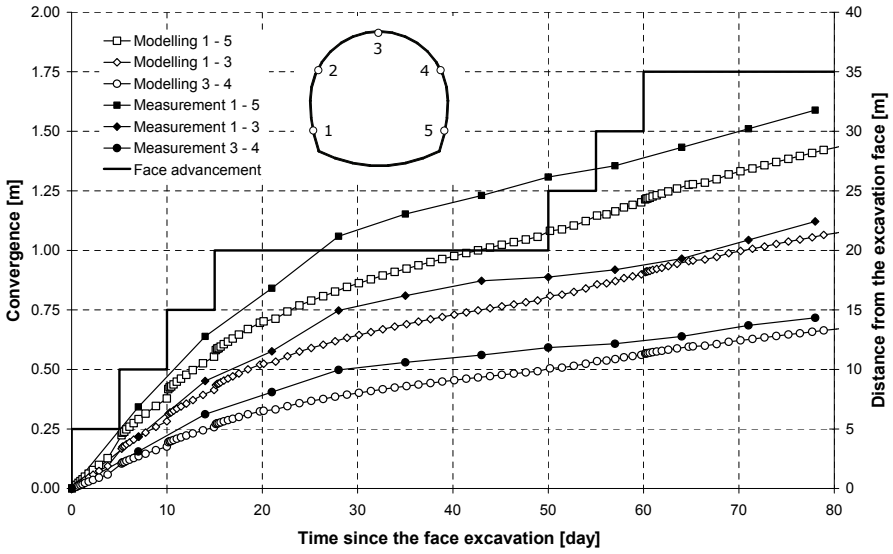

Figure 5: Convergence versus time in section C for different directions: comparison between numerical results and the measured data

the concrete lining, using the rock constitutive model whose parameters were previously calibrated versus in-situ measurements. This was achieved in blind conditions before completion of the work.

Modelling the interaction between the support and the rock mass required special attention (Cantieni and Anagnostou, 2009a; Carranza-Torres and Diederichs, 2009). In this computation a concrete lining was installed 10 meters from the excavation face. The lining thickness was 1.0 meter. The Young's modulus and Poisson's ratio of the concrete were 20 GPa and 0.3, respectively. Figure 6 shows the evolution with respect to time of the radial displacement of the tunnel wall. As a comparison, the radial displacement for the unsupported drift is also reported.

3.3.1 Stress distribution around the drift

The evolution of the stress at the contact between the lining and the rock mass is shown in Figure 7. At the start, the radial stress was zero at the tunnel wall because of the excavation. After the concrete lining was installed (10 days) the radial stress increased gradually to reach 5 MPa after 150 days; however, this value is still less than the initial stress (7.5 MPa).

Different profiles of the orthoradial stress corresponding to different times are presented in Figure 8. Immediately after the excavation, the rock surrounding the drift

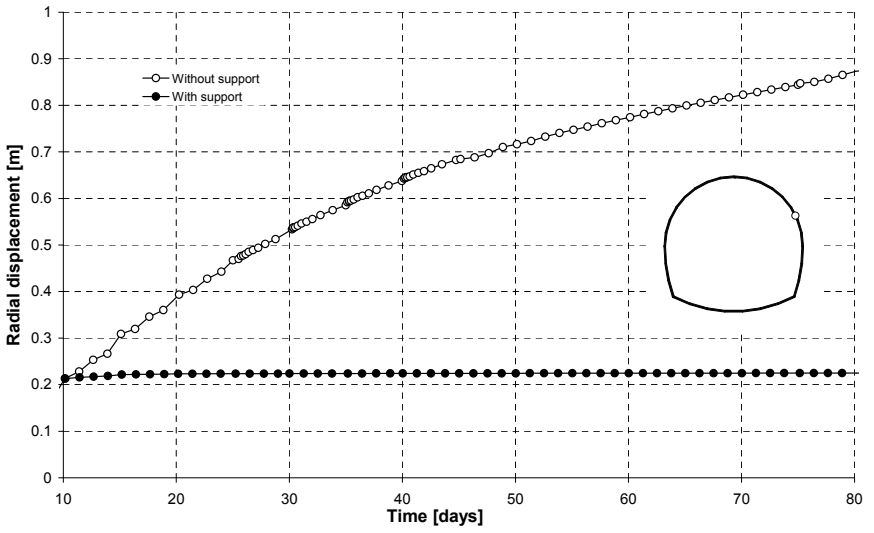

Figure 6: Radial displacement versus time for supported and unsupported drift

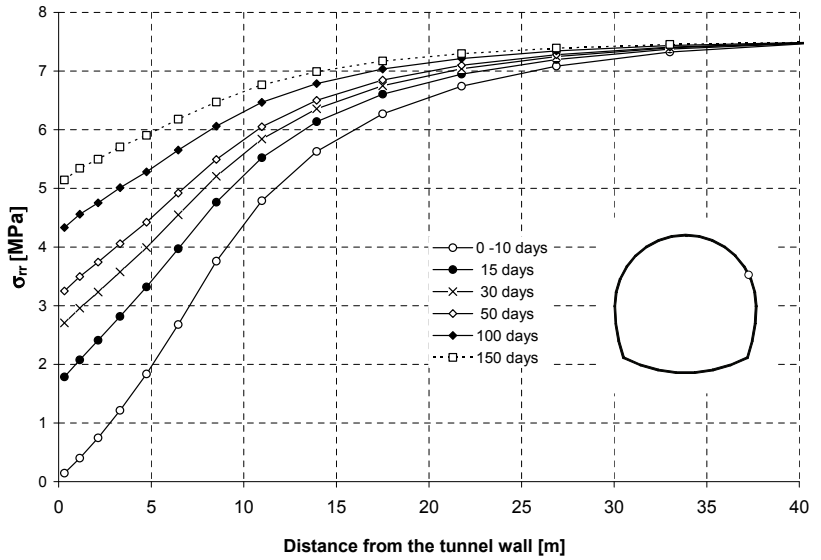

Figure 7: Distribution of radial stress with respect to the distance to the drift wall at different times after the concrete lining support was installed

exhibited plastic behaviour. The extension of the plastic zone was approximately 8 meters. Ten days after the excavation was completed the lining support was installed. Therefore the maximum orthoradial stress started to decrease because of time-dependent damage and stress relaxation. On the other hand, at the drift wall, the orthoradial stress starts to increase because of contact with the concrete lining, which provided a confining pressure.

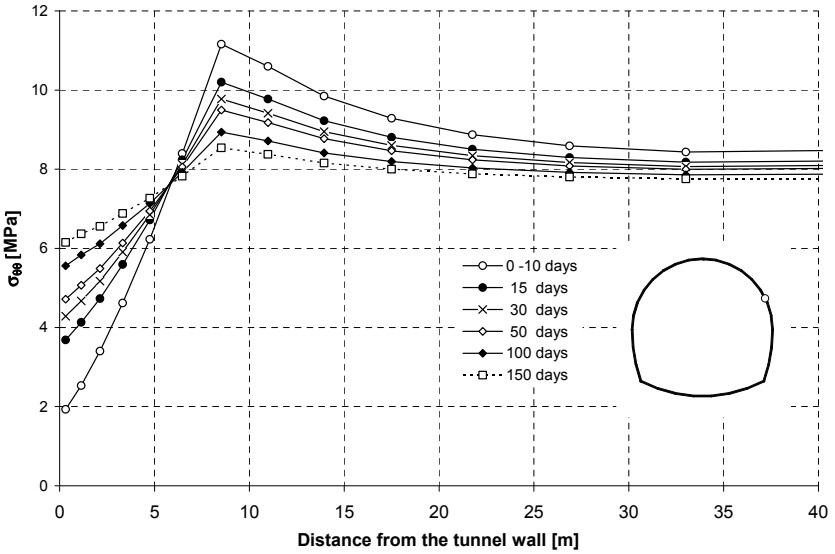

Figure 8: Distribution of orthoradial stress with respect to distance to the drift wall at different times after the concrete lining support was installed

3.3.2 Stress path at the contact between the rock and the concrete liner

The progressive mobilization of the stress at the contact between the rock and the concrete liner was analysed by Pellet and Roosefid (2007) as well as by Cantieni and Anagnostou (2009b) and Sandrone and Labiouse (2009). Figure 9 shows the stress history from the initial state of stress to the final equilibrium for different constitutive models, namely elastoplastic, and elasto-viscoplastic (CVISC) with and without support. For the case under study (CVISC with support), the computations show that the radial stress decreases to zero after excavation. Subsequently, after excavation but before installation of the lining support, the rock creeps and viscoplastic deformations take place. After the concrete lining support installation, the radial stress progressively increases until equilibrium is reached. It has to be

noted that before lining installation the two numerical simulations (with and without support) do not give the same displacement, as might be expected. This is due to the fact that in the present case, the drift is excavated and supported in stages. Therefore the displacement in the unsupported section, before installation of the lining, is affected by the sections that are already supported and located behind the unsupported section.

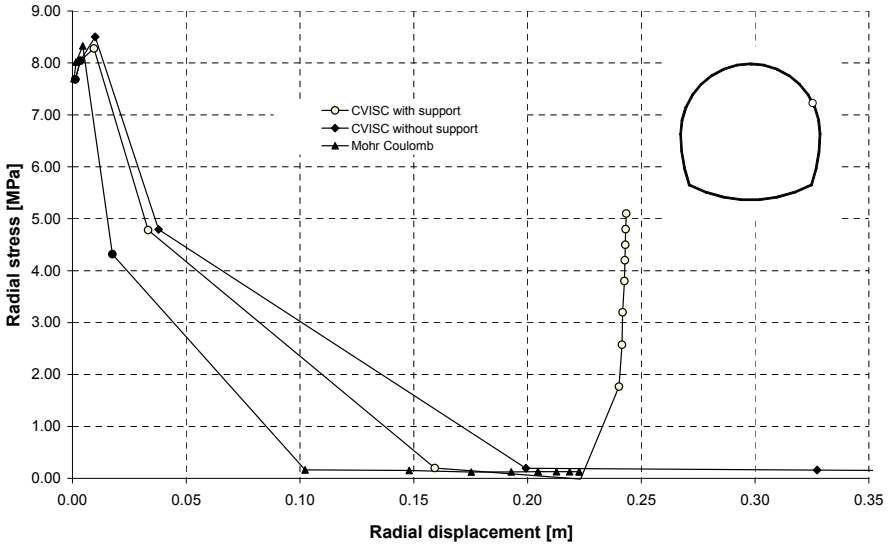

Figure 9: Radial stress at the contact between the concrete lining support and rock mass versus radial displacement for different situations

The evolution of the orthoradial stress in the lining with respect to time was analysed. After 80 days, normal stress reached about 35 MPa at the intrados of the lining and 5 MPa at the extrados (Figure 10). The average maximum normal stress is 18 MPa which is somewhat greater than the 14 MPa measured in the lining (Rettighieri et al., 2008).

4 Conclusion

In this paper it was shown that the time-dependent behaviour of a drift excavated in a soft rock can be properly modelled using a viscoplastic damageable constitutive equation. In this numerical simulation, all the construction sequences were taken into account, including the stages of tunnel excavation and the contact with the concrete lining support.

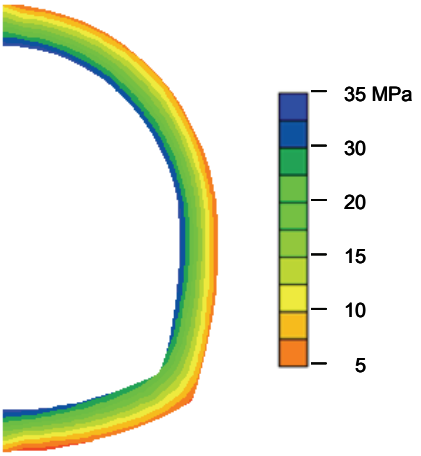

Figure 10: Normal stress distribution in the concrete lining support 80 days after its installation

The calibration of the constitutive parameters used in the computation was achieved with the simulation of a lightly supported section; this aimed to fit the computed displacements to the measured displacements. The critical parameter identified is the rock viscosity because it may vary with the state of stress. For Kelvin viscosity, the order of magnitude is consistent with the values proposed in the literature for this kind of rock. In addition, it is shown that the parametrical values are of the order of magnitude range of those assessed using rock mass classification systems. Nevertheless, the choice of appropriate values to account for the scale effects is still the key point of such analysis, especially for rock dilation angle and rock viscosity.

As expected, the contact between the lining support and the rock mass drastically slows and finally stops the drift closure. The predictions of the stresses acting in the concrete lining are close to those that were measured. Overall, the analysis, achieved under blind conditions, provided a good average maximum value of the final stress in a concrete lining and therefore proved to be an appropriate tool for the design of the drift support system.

References

Boidy, E., Bouvard, A., Pellet, F. (2002): Back analysis of time-dependent behaviour of a test gallery in claystone, *Tunnelling and Underground Space Technology*, vol 17: 415-424.

Cantieni, L., Anagnostou, G. (2009a): The interaction between yielding supports

and squeezing ground, *Tunnelling and Underground Space Technology,* vol 24: 309-322.

Cantieni, L., Anagnostou, G. (2009b): The effect of the stress path on squeezing behavior in tunneling, *Rock Mechanics and Rock Engineering*, vol 42: 289-318.

Carranza-Torres, C., Diederichs, M. (2009): Mechanical analysis of circular liners with particular reference to composite supports: For example, liners consisting of shotcrete and steel sets, *Tunnelling and Underground Space Technology*, vol 24: 506-532.

Cormeau, I. (1975): Numerical stability in quasi-static elasto-viscoplasticity, *International Journal for Numerical Methods in Engineering*, vol 9: 109-127.

Dhawan, K.R., Singh, D.N., Gupta, I.D. (2002): 2D and 3D finite element analysis of underground openings in an inhomogeneous rock mass, *International Journal of Rock Mechanics and Mining Sciences,* vol 39: 217–227.

Dinis, L.M.J.S., Natal Jorge, R.M., Belinha, J. (2009): Large deformation applications with the radial natural neighbours interpolators, *CMES: Computer Modeling in Engineering & Sciences*, vol. 44, no. 1: 1-34.

Eberhardt, E. (2001): Numerical modelling of three-dimension stress rotation ahead of an advancing tunnel face, *International Journal of Rock Mechanics and Mining Sciences*, vol 38:499–518.

Fabre, G., Pellet, F. (2006): Creep and time dependent damage in argillaceous rocks, *International Journal of Rock Mechanics and Mining Sciences*, vol 43: 950-960.

Han-Ping Chin, J., Rogers, J.D. (1987): Creep parameters of rocks on an engineering scale, *Rock Mechanics and Rock Engineering*, vol 20: 137-146.

International Society of Rock Mechanics (2007): The complete ISRM suggested methods for rock characterization, testing and monitoring, Ulusay and Hudson Editors, ISRM.

Korzeniowski, W. (1991): Rheological model of hard rock pillar, *Rock Mechanics and Rock Engineering*, vol 24: 155-166.

Kropik, C., Mang, H.A. (1996): Computational mechanics of the excavation of tunnels, *Engineering Computations*, vol 13: 49-69.

Luming, S. (2009): A rate-dependent damage/decohesion model for simulating glass fragmentation under impact using the material point method, *CMES: Computer Modeling in Engineering & Sciences*, vol. 49, no. 1: 23-46.

Marti, J., Cundall, P.A. (1980): Mixed discretization procedures for accurate solution of plastic collapse, *International Journal for Numerical and Analytical Methods in Geomechanics*, vol. 6: 129-139.

Pellet, F., Roosefid, M., Deleruyelle, F. (2009): On the 3D numerical modelling of the time-dependent development of the Damage Zone around underground galleries during and after excavation, *Tunnelling and Underground Space Technology*, vol. 24: 665-673.

Pellet, F., Roosefid, M. (2007): Time dependent behaviour of rock and practical implications to tunnel design, *Proc. 11th International Congress on Rock Mechanics*, Lisbon, Portugal: 1079-1082.

Pellet, F., Hajdu, A., Deleruyelle, F., Besnus, F. (2005): A viscoplastic constitutive model including anisotropic damage for the time dependent mechanical behaviour of rock, *International Journal for Numerical and Analytical Methods in Geomechanics*, vol 29: 941-970.

Rettighieri, M., Triclot, J., Mathieu, E., Barla, G., Panet, M. (2008): Difficulties associated with high convergences during excavation of the Saint Martin La Porte access adit, *Proc International Congress, Building Underground for the Future*, AFTES, Monaco: 395-403.

Russo, G., (2009): A new rational method for calculating the GSI, *Tunnelling and Underground Space Technology*, vol. 24: 103-111.

Russo, G., Repetto, L., Piraud J., Laviguerie, R. (2009): Back-analysis of the extreme squeezing conditions in the exploratory adit to the Lyon-Turin base tunnel, *Proc. RockEng09, Rock engineering in difficult conditions*, Toronto, Canada: 156-165.

Sandrone, F., Dudt, J.P., Labiouse, V, Descoeudres, F. (2006): Analysis of delayed convergences in a carbon zone of the Lötschberg tunnel, *Proc. Eurock Conference,* Liege, Belgium:351-356.

Sandrone, F., Labiouse, V. (2009): Analysis of the evolution of road tunnels equilibrium conditions with a convergence–confinement approach, *Rock Mechanics and Rock Engineering*, vol 44: in press.

Selvadurai, A.P.S. (2004): Stationary damage modelling of poroelastic contact, *International Journal of Solids and Structures*, vol 41: 2043–2064.

Sladek, J., Sladek, V., Solek, P. (2009): Elastic analysis in 3D anisotropic functionally graded solids by the MLPG, *CMES: Computer Modeling in Engineering & Sciences*, vol. 43, no. 3: 223-252.

Sterpi, D., Gioda, G. (2009): Visco-plastic behaviour around advancing tunnels in squeezing rock, *Rock Mechanics and Rock Engineering*, vol 42: 319-339.

Sulem, J., Panet, M., Guenot, A. (1987): An analytical solution for time-dependent displacements in a circular tunnel, *International Journal of Rock Mechanics and Mining Sciences*, vol. 24: 155-164.

Tan, C. L., Shiah, Y.C., Lin, C.W. (2009) Stress analysis of 3D generally anisotropic elastic solids using the boundary element method, *CMES: Computer Modeling in Engineering & Sciences*, vol. 41, no. 3: 195-214.

Triclot, J., Rettighieri, M., Barla, G. (2007): Large convergences observed in the Saint Martin La Porte access gallery to the Lyon-Torino base tunnel, *Tunnels et Ouvrages souterrains*, no. 204: 409-413.